APPLICATION OF THE MACH WAVE ELIMINATION METHOD TO SUPERSONIC JET ENGINES

Marco Debiasi* and Dimitri Papamoschou †
Department of Mechanical and Aerospace Engineering
University of California, Irvine
Irvine, CA 92697-3975

Abstract

We report noise measurements for supersonic jets surrounded by a coflow at conditions that prevent emission of Mach waves and discuss application of this silencing technique to engines of supersonic business and military aircraft. Several jet and coflow combinations, suitable for Mach wave elimination and compatible from an engine cycle point of view, were explored. Far-field noise spectra demonstrate that application of the coflow reduces noise up to 16 dB in the direction of strongest emission at the frequencies to which humans are more sensitive. Reduction of the same spectral components in the lateral direction ranged from 5 to 8 dB. A preliminary analysis of the Brayton-Joule cycle indicates that a turbofan engine with jet and coflow conditions for Mach wave elimination is feasible using current technologies. Engines for supersonic business aircraft that apply this method could be designed around the core of current military turbofan engines.

I. Introduction

Interest has been shown lately for the development of supersonic business aircraft. Dassault Aviation disclosed plans for a Mach 1.8 business jet during the 1998 National Business Aviation Association. Lockheed and Gulfstream Aircraft announced the study of a similar airplane. This is an indication that, in spite of the higher acquisition and operational costs compared to their subsonic counterparts, supersonic business jets can have a niche in a market where time saving often translates in crucial financial benefits.

---

*Graduate Student, member AIAA
†Professor, member AIAA
0

Development of a supersonic business aircraft would leverage the extensive know-how and technologies developed for military aircraft.

The development of commercial supersonic aircraft hinges on efficient reduction of take-off noise generated by hot supersonic jets exhausting from the high-performance engines of such aircraft. Untreated, these jets create noise levels well above those permitted by current Federal Aviation regulations (FAR 36 Stage III). Military aircraft may also need to become quieter to conform to community noise regulations and for stealth advantage. Several theoretical, numerical and experimental studies [1, 2, 3, 4, 5, 6] recognized that an important contribution to the elevated noise of jet engines is due to Mach waves. In addition to Mach-wave noise, high-level acoustic emissions (screech and broadband noise) also occur in jets with strong shocks, i.e., in under- or over-expanded jets.

Recently it has been shown by Papamoschou that surrounding a supersonic jet with a coflow of proper characteristics inhibits the formation of Mach waves [7, 8]. The principle underlying this technique, named Mach Wave Elimination (MWE), is to make the jet and the coflow eddy convective velocities subsonic with respect to their surrounding streams. An empirical model for the required coflow properties is based on direct measurements of the eddy convective velocity in supersonic shear layers and round jets [9]. Schlieren photographs have shown that the method is effective in preventing formation of Mach waves in supersonic jets [7]. Microphone surveys [10] showed that Mach waves are the principal noise contributors in the near field and that in the far field they constitute at least 85% of the sound to which humans are most sensitive. The experiments also indicated that surrounding a high-speed jet with a coflow of appropriate Mach number and temperature reduces noise substantially. Subsequent experiments in over-

and under-expanded high-speed jets [11] provided a better understanding of the dependence of noise characteristics of high-speed jets on jet and coflow conditions and proved the value of the coflow in reducing the Mach wave noise in imperfectly-expanded jets.

Since the MWE method utilizes propulsive means to prevent generation of Mach waves, in contrast to existing techniques that use intrusive devices to suppress or confine Mach waves after they are formed, it should be of great utility to engine manufacturers and airframe builders developing supersonic transports. The purpose of the present work is to show the applicability of the MWE method to the design of jet engines intended to power a supersonic business aircraft. To this aim, the noise field of appropriate jet and coflow combinations has been studied. A preliminary analysis of the corresponding Brayton-Joule cycle has been used to validate the jet and coflow conditions from a thermodynamic point of view and to assess the performance of an engine that applies the MWE method and is derived from a military turbofan.

II. Principle of Method

Mach waves are generated by turbulent eddies that propagate in the jet with convective velocity U_c supersonic with respect to the surrounding air stream, as sketched in Fig. 1. The principle of Mach Wave Elimination is to make all the eddy motions subsonic with respect to their surrounding streams by encircling the jet exhaust with a suitable layer of coflowing gas (Fig. 2). In the analysis that follows, subscript 1 denotes the jet properties, 2 the coflow properties, and ∞ the ambient air-stream properties. The symbol U represents the flow velocity, a the speed of sound, $M = U/a$ the Mach number and U_c the eddy convective velocity. Thus, to prevent generation of Mach waves, the following relations must be satisfied

$$U_{c_1} - U_2 < a_2$$
$$U_{c_2} - U_\infty < a_\infty \tag{1}$$

These relations can also be cast in terms of the convective Mach number of the eddies with respect to the low-speed side, commonly referred to as M_{c2} (M_{c1} being the convective Mach number with respect to the high-speed side). Here it is required that

$$M_{c2_1} < 1$$
$$M_{c2_2} < 1 \tag{2}$$

An empirical model for M_{c2} [12, 9] translates Eqn. 2 into practical requirements for the Mach number

M_2 and static temperature T_2 of the coflow. These requirements are plotted in Fig. 3 for $M_1 = 1.2$, $T_1/T_\infty = 2.5$ with $M_\infty = 0$. In this figure the lower curve represents conditions at which $M_{c2_1} = 1$ and in the region below this curve Mach waves originate from the jet. The upper curve represents conditions at which $M_{c2_2} = 1$ and in the region above this curve Mach waves originate from the coflow. Mach Wave Elimination occurs in the region bounded by the two curves. In a separated-flow turbofan engine, there are two basic options of applying this technique: (a) adjusting the fan compression ratio; (b) adding heat to the fan stream. This study investigates the first option.

III. Experimental Apparatus

Experiments were conducted in a coaxial jet facility described in detail in [7]. Mixtures of helium and air were supplied to a concentric nozzle arrangement as shown in Fig. 4. The inner nozzle, of 12.7 mm exit diameter, was designed by the method of characteristics for Mach number $M_1 = 1.5$. The outer nozzle formed a smooth contraction terminating in an exit diameter of 17.8 mm and 21.6 mm. Precisely-metered mixtures of helium and air were supplied to the nozzles, which exhausted into ambient, still air. The stagnation pressure of the jet and coflow were maintained within 1% of the value needed to obtain the required degree of expansion at the nozzle exit. Helium-air mixtures duplicate accurately the density, velocity, and speed of sound of a heated jet. By regulating the mass fractions of helium and air, thereby regulating the gas constant of the mixture, we controlled the jet velocity at a fixed Mach number. The density of the mixture can be translated to the effective temperature of a heated jet via the relation $\rho_\infty/\rho = T/T_\infty$, where ∞ refers to the ambient conditions.

Table 1 summarizes the jet conditions covered in this paper. The first column indicates the cases studied; the following two columns provide the values of the perfectly-expanded jet Mach number M_1 and velocity U_1 assumed by the jet stream after external compression to match the ambient pressure. Next are two columns providing the values of the coflow Mach number M_2 and velocity U_2. The last column indicates the calculated ratio of the overall thrust and the thrust of a $M_1 = 1.5$, $U_1 = 920$ m/s jet, which has been used here and in [10, 11] as the reference thrust.

Table 1. Jet Flow Conditions

Case	M_1	U_1	$\frac{D_2}{D_1}$	M_2	U_2	$\frac{F}{F_{ref}}$
A	1.20	700	0	0	0	0.72
B	1.20	700	1.4	0.80	300	0.99
C	1.20	700	1.4	1.00	350	1.12
D	1.22	700	1.7	0.80	300	1.28
E	1.20	700	1.7	1.00	350	1.47
F	1.20	630	0	0	0	0.69
G	1.20	630	1.4	0.80	300	0.97
H	1.20	630	1.4	1.00	350	1.10
I	1.00	450	0	0	0	0.79

U in m/s

IV. Sound Measurement

The noise measurement method is summarized in Fig. 5. Noise was recorded with a one-eighth inch condenser microphone (Brüel & Kjær 4138), with a frequency response up to 150 kHz, inside an anechoic chamber. The microphone was mounted on an arm which pivoted around an axis passing through the center of the jet exit. This arrangement enabled sound measurements at a variety of radial (r) and azimuthal (θ) positions with r ranging from 0.038 to 1.52 m and θ ranging from 20° to 100°, measured counter-clockwise from the jet axis. The signal was high-pass filtered at 500 Hz by a Butterworth filter to remove spurious low-frequency noise. The power spectrum of each recording was computed using a 512-point FFT with a full Hanning window.

Signal processing yielded two important noise parameters, the sound pressure level (SPL) spectrum which shows the distribution of noise versus frequency and the overall sound pressure level (OASPL) which describes the total noise at a given point. The units for both quantities are decibels (dB). The SPL spectrum is given by

$$\text{SPL}(f) = 10 \log_{10} S(f) \qquad (3)$$

where $S(f)$ is the properly-normalized power spectrum of $p'_{\text{rms}}/p_{\text{ref}}$, the pressure fluctuation relative to reference pressure $p_{\text{ref}} = 20 \ \mu\text{Pa}$. The OASPL can be computed in the frequency domain by

$$\text{OASPL} = 10 \log_{10} \int_{0 \ \text{Hz}}^{150 \ \text{kHz}} S(f) df \qquad (4)$$

where the upper limit of integration is dictated by the highest frequency response of the microphone. Another important quantity is the value of the SPL spectrum at $f = 100$ kHz, denoted $\text{SPL}_{100\text{-kHz}}$. Considering that our jet is 1/50 to 1/100 scale, a frequency of 100 kHz measured in our experiment corresponds to 1000-2000 Hz in a full-scale engine, i.e., the frequency range of most annoying to humans. The 100-kHz component is defined here as the average spectral value of the bandwidth 100 ± 13 kHz and is computed as

$$\text{SPL}_{100\text{-kHz}} = 10 \log_{10} \left[\frac{1}{\Delta f} \int_{f_0 - \Delta f/2}^{f_0 + \Delta f/2} S(f) df \right] \quad \text{(dB)} \qquad (5)$$

with $f_0 = 100$ kHz and $\Delta f = 26$ kHz. Before calculating these quantities using Eqs. 3, 4 and 5, the microphone signal was corrected for its frequency and the free-field response as explained in [10]. Meaningful comparison of jets requires the evaluation of the noise characteristics at equal thrust while preserving the physics of each case. To this end, all the spectra are scaled to equal thrust using standard geometric scaling procedures [10]. For each case the correction in terms of SPL is

$$\Delta\text{SPL} = -10 \log_{10} \left(\frac{F}{F_{ref}} \right) \qquad (6)$$

The same correction applies to the OASPL data. It is important to recall that the thrust correction is based solely on measured noise data and that no assumptions, such as a power-law dependence of sound intensity on velocity, are involved.

The spectra are plotted versus the Strouhal number, $\text{St} = f D_1 / U_1$. To relate our results to a full-scale engine with exit diameter of 0.5 m, the full-scale frequency is given approximately by

$$f_{\text{full-scale}} \approx 2 \text{ St } U_1 \qquad (7)$$

For velocities in the range of 700 m/s, spectral components below $\text{St} = 0.35$ correspond to $f_{\text{full-scale}} \leq 500$ Hz, thus are not very significant to noise perceived by humans. Further details of the acoustic measurement setup can be found in [10].

V. Brayton-Joule Cycle Analysis

A preliminary evaluation of the most important thermodynamic values for the Brayton-Joule cycle of a jet engine incorporating the MWE method follows the criteria presented in [13]. Fig. 6 represents the Brayton-Joule cycle for a turbojet/turbofan engine and indicates the processes the gas undergoes in the various engine components. In the following analysis

subscript 0 refers to stagnation values and subscript S refers to values obtained isentropically. Additional subscripts are used to indicate the engine components and the corresponding quantities.

To compare results relative to different cycles using the same engine core, it is proper to non-dimensionalize the mass flow rates in each component with respect to the mass flow rate in the compressor. The mass ratio between the generic mass flow rate $\dot{m}$ and the mass flow rate $\dot{m}_{com}$ in the compressor is defined as

$$m_r = \frac{\dot{m}}{\dot{m}_{com}} \tag{8}$$

So, for instance, the bypass ratio BPR is equal to

$$BPR = m_{r_{fan}} = \frac{\dot{m}_{fan}}{\dot{m}_{com}} \tag{9}$$

Variations of specific heat c_p and c_v and their ratio γ during a process are considered negligible. In this hypothesis, the efficiency η_c and η_e of the generic compression and expansion processes are defined as

$$\eta_c = \frac{T_{0_{f,S}} - T_{0_i}}{T_{0_f} - T_{0_i}} \tag{10}$$

$$\eta_e = \frac{T_{0_f} - T_{0_i}}{T_{0_{f,S}} - T_{0_i}} \tag{11}$$

where the subscripts i and f indicate the initial and final state of the process. The efficiency η_h of the generic heating process is defined as

$$\eta_h = \frac{\left(m_{r_f} T_{0_f} - m_{r_i} T_{0_i}\right) c_p}{m_{r_{fuel}} Q} \tag{12}$$

where Q is the heating value of jet A fuel ($Q = 43,400$ kJ/kg). Other important formulas used in the analysis are the isentropic formulas relating the Mach number to the stagnation and static properties. Typical values of component efficiency and gas specific heat ratio, suggested in [13] and summarized in Table 2, were used for the processes in the various engine components. Once we select the fan and overall pressure ratios, the maximum temperature at the turbine entrance, and the ambient conditions upstream of the engine, the equations above can be combined to compute the values of stagnation and static temperature and pressure and the mass ratio at each point of the cycle.

Table 2. Parameters for Brayton-Joule components

Component	Adiabatic efficiency	Average specific heat ratio γ
air intake	$\eta = 0.97$	1.40
fan	$\eta = 0.85$	1.40
compressor	$\eta = 0.85$	1.37
combustor	$\eta = 1.00$	1.35
turbine	$\eta = 0.90$	1.33
jet nozzle	$\eta = 0.98$	1.36
fan nozzle	$\eta = 0.97$	1.4

The temperature at the turbine exit is obtained by equating the power produced by the turbine to the power needed to drive the compressor and the fan. Knowing the temperature values at the fan and turbine exit and imposing the Mach number at the jet and fan nozzle exit, one can compute the stagnation and static parameters of the stream at these locations. If the fan and core stream are mixed prior to expansion in the jet nozzle, the conditions upstream of the nozzle are obtained by treating the mixing process as adiabatic. The mass ratio of the mixed stream is then the sum of the fan and turbine mass ratios and its specific heat is obtained by mass-averaging those of the fan and turbine streams. The mixed stream temperature is obtained from the adiabatic condition for the mixing process while the stagnation pressure drop is a function of the entropy increase in that process. The equations for the exit area of the jet and fan nozzle are

$$A_1 = \frac{\pi D_1^2}{4} = \frac{\dot{m}_1}{\rho_1 U_1} = \frac{\dot{m}_{com} m_{r,1}}{\rho_1 U_1} \tag{13}$$

$$A_2 = \frac{\pi D_2^2}{4} - A_1 = \frac{\dot{m}_2}{\rho_2 U_2} = \frac{\dot{m}_{com} m_{r,2}}{\rho_2 U_2} \tag{14}$$

The overall thrust F of the engine is

$$F = F_1 + F_2 = \begin{aligned} &\dot{m}_1 U_1 + A_1 (p_1 - p_\infty) + \\ &\dot{m}_2 U_2 + A_2 (p_2 - p_\infty) - \dot{m}_\infty U_\infty \end{aligned} \tag{15}$$

which, cast in terms of mass ratio and introducing Eqs. 13 and 14, gives the value of the engine specific thrust ST

$$ST = \frac{F}{\dot{m}_{com}} = \begin{aligned} &m_{r,1}\left(U_1 + \frac{p_1 - p_\infty}{\rho_1 U_1}\right) + \\ &m_{r,2}\left(U_2 + \frac{p_2 - p_\infty}{\rho_2 U_2}\right) - \\ &m_{r,\infty} U_\infty \end{aligned} \tag{16}$$

from which the overall thrust F corresponding to a specified value of the compressor mass flow rate $\dot{m}_{com}$

is obtained as

$$F = ST\, \dot{m}_{com} \qquad (17)$$

Then, the generic mass flow rate $\dot{m}$ in any component and point of the cycle can be computed with

$$\dot{m} = m_r\, \dot{m}_{com} \qquad (18)$$

The diameters D_1 and D_2 of the jet and coflow nozzles can be derived from Eqs. 13 and 14. Similarly, the dimension of other engine components can be derived once we know the corresponding local values of the mass flow rate, density and velocity. Finally, the Specific Fuel Consumption SFC is computed as

$$SFC = \frac{\dot{m}_{fuel}}{F} \qquad (19)$$

The analysis of the Brayton-Joule cycle described above has been implemented in a computer routine. Iterations were performed changing the fan and overall pressure ratio and the maximum cycle temperature until bypass, compressor mass flow rate and nozzle conditions matched specified values.

VI. Results

Noise Measurements

It has already been demonstrated by the authors that noise radiated in the aft quadrant depends principally on the perfectly-expanded values of the Mach number M_1 and velocity U_1 in the jet plume [11]. In the same work, the effect of these two parameters on the emission of Mach waves and on their elimination using a coflow was analyzed. It was found that the best noise reduction associated to the elimination of Mach waves is obtained for velocities U_1 in the range 600-700 m/s. Decreasing M_1 while maintaining U_1 unchanged leads to an additional noise reduction in the high-frequency components. Another important parameter influencing the reduction of noise, also taken into account in this study, is the thickness of the coflow annulus. Clearly, the larger this value, the more effective is the coflow, but the larger becomes the bypass ratio required to generate it, a limiting factor in designing a supersonic engine.

We discuss now the noise characteristics of the flow conditions of Table 1. For some of the cases, the far-field SPL spectra, whose values represent characteristics of noise perceived by airport communities, are presented. The spectra refer to the OASPL peak direction (the direction of strongest noise emission)

and to the lateral direction. The most relevant acoustic results for all the cases are summarized in Table 3. The spectra and all the other data are always presented after correction for equal thrust.

Table 3 Far-field noise at $r/D_1 = 80$ in the peak emission and lateral direction

Case	OASPL peak	SPL at 100 kHz peak	OASPL lateral	SPL at 100kHz lateral
A	130.53	64.73	114.54	57.47
B	127.92	58.54	111.43	53.42
C	127.94	55.49	110.95	51.92
D	125.73	48.51	111.91	51.57
E	128.00	55.82	111.85	49.93
F	128.05	61.23	112.42	54.94
G	125.51	54.39	108.77	50.63
H	125.70	51.84	108.94	49.21
I	126.41	58.45	112.26	55.24

OASPL and $SPL_{100\text{-kHz}}$ in dB

Fig. 7 (a) represents the spectra at the OASPL peak direction ($\theta = 40^o$) of untreated jet Case A with $M_1 = 1.2$ and $U_1 = 700$ m/s and of the same jet treated using a coflow with $M_2 = 0.8$, $U_2 = 300$ m/s and $D_2/D_1 = 1.4$ (Case B). Application of the coflow produces the typical noise reduction observed in previous investigations. That is, moderate noise reduction at low Strouhal numbers and significant noise reduction at higher values, especially in the range ($St = 1.5 - 2.5$) more relevant to full-scale engine noise. At these frequencies, the noise reduction achieved with the coflow is about 7 dB. Fig. 7 (b) represents the spectra of Cases A and B in the lateral direction ($\theta = 90^o$). In this direction the noise reduction with application of the coflow is rather uniform throughout the frequency range. The reduction at medium-to-high frequencies (about 5 dB) could still be partially ascribed to the elimination of Mach waves which, at high angles, produce weak spherical waves propagating radially. Very similar results, not shown here, were obtained for the same jet using a coflow with $M_2 = 1.0$ and $U_2 = 350$ m/s and same nozzle diameter ratio as the previous case (Case C).

Fig. 8 represents the spectra of untreated jet Case A and of treated jet Case D, i.e. the same jet treated using a coflow with Mach number and velocity equal to those of Case B but larger diameter $D_2/D_1 = 1.7$. The same figure also represents the spectra of Case I which is a jet with $M_1 = 1.0$ and $U_1 = 450$ m/s obtained mixing the jet and coflow of Case D before exhausting from the jet nozzle. Fig. 8 (a) shows clearly the acoustic benefit of using a larger diameter coflow which, at the peak OASPL angle, produces better noise reduction at all the frequency compo-

nents and a reduction of about 16 dB in the range $St = 1.5 - 2.5$. In the same figure it is seen that mixing the coflow and primary stream to lower the exit velocity is a less effective means for silencing the jet. In the range $St = 1.5 - 2.5$, noise reduction for mixed Case I is about 5 dB compared to 16 dB for the unmixed Case D. The noise reduction in the lateral direction also benefits from the larger coflow even though the decrease in this direction is less dramatic (6 dB at the medium-to-high frequencies). In this direction, the over-expanded mixed jet Case I exhibits strong screech tones and does not show any acoustic benefit even if these tones are discounted.

Increasing the coflow Mach number to $M_2 = 1.0$ (Case E), produces a noise reduction in the peak OASPL direction midway between those of Cases B and D (Fig. 9(a)) and a noise reduction in the lateral direction which is slightly better than Case C (about 8 dB at $St = 1.5 - 2.5$, Fig. 9(b)). Cases G and H represent the application of the same coflow of Cases B and C to a lower speed jet (Case F with $U_1 = 630$ m/s) and produced spectra, not shown here, similar to those of Cases B and C.

These results indicate that maintaining separated the fan and core streams at Mach Wave Elimination conditions is acoustically superior to mixing these streams internally before expansion. A certain flexibility exists in the choice of coflow conditions that deliver good noise reduction.

Engine performance analysis

A preliminary estimate of the performance of a turbofan engine for supersonic business aircraft which exploits the MWE method at take-off is presented.

As a baseline, we refer to a twin-engine supersonic airplane jet with maximum take-off weight of about 65,000 lb. Engines for this aircraft could be designed around the core of current military turbofans in the class 11,250 lbf dry-thrust at sea-level. Typically, these engines have a bypass ratio $BPR \approx 0.5$, overall pressure ratio $OPR \approx 25$, maximum turbine entrance temperature $TET \approx 1800$ K and core mass flow rate about 90-110 lb/s. Modifications would require the substitution of the rotors in the first fan stages with larger ones to generate the increased bypass stream required for the coflow and the use of smaller rotors in the remaining fan stages to accommodate the original core mass flow rate. At take-off, the fan and core streams should remain separated using the coaxial arrangement exemplified by Fig. 10 (a). During other segments of the mission, the mixed fan and core streams would expand through the adjustable converging-diverging jet nozzle. This requires a variable-cycle engine where the fan and core streams are mixed at some point in the cycle. Two extreme configurations are the following: i) the fan and core streams are mixed upstream of the jet nozzle as sketched in Fig. 10 (b); ii) the fan stream is diverted into the compressor- this is equivalent to converting the turbofan to a pure turbojet (Fig. 10 (c)).

Table 4 summarizes the performance at different flight conditions and other important parameters pertaining to the cycle analysis of section V. The first column identifies the quantities shown in the table. The second and third columns represent the take-off parameters of engines whose jet and coflow have characteristics of Case D and E respectively, i.e. the most effective conditions for take-off noise suppression. The next two columns represent the cruise parameters (at altitude 53,000 ft and Mach 1.8) of the mixed-stream turbofan and of the same engine converted to a turbojet. The last two columns represent, for the same engines, the parameters at typical transonic acceleration conditions. Since similar values have been found at cruise and transonic acceleration for $FPR = 1.7$ and $FPR = 2.1$, the data in the last four columns refer to the lower fan pressure ratio (Case D at take-off conditions).

The TET values for all the conditions are in the range permitted by current turbine-cooling techniques. At take-off, two Case D engines develop a thrust of about 24,600 lbf, enough for a 65,000 lb aircraft with take-off $L/D \approx 5$. This thrust is obtained without reheat of the exhausting streams. Due to its high bypass, the take-off SFC is 0.54 lb/lbf h, less than the typical value 0.75 lb/lbf h for a military turbofan with the same core. The diameter D_2 of the coflow nozzle is less than 1 m, an acceptable dimension for supersonic engines. Engine Case E exhibits take-off properties similar to those of Case D. The principal difference is the higher TET needed for generating the higher pressure coflow of Case E. This also results in a higher take-off thrust at same core mass flow rate. One should remember that this higher thrust does not translate to any acoustic benefits, since at equal thrust the noise reduction of Case E is less than that of Case D. In actuality, at take-off, Case E engine is noisier than Case D and appears to be a convenient option only for heavier aircraft.

At cruise, the fan stream can be diverted and mixed with the core stream by opening a section of the core duct upstream of the jet nozzle as shown in Fig. 10 (b). The mixed streams expand in the adjustable jet nozzle which, in these conditions, can be fully opened filling the coflow annulus gap. To achieve maximum expansion, the exit diameter of the jet nozzle can be-

Table 4.   Parameter of MWE engines at different flight conditions

	Case D take-off	Case E take-off	mixed-stream cruise	turbojet cruise	mixed-stream transonic	turbojet transonic
M_∞	0.0	0.0	1.8	1.8	1.2	1.2
Altitude ft (m)	0 (0)	0 (0)	53,000 (16,000)	53,000 (16,000)	40,000 (12,000)	40,000 (12,000)
Temperature R (K)	540 (300)	540 (300)	396 (220)	396 (220)	396 (220)	396 (220)
BPR	2.3	2.3	2.3	0.0	2.3	0.0
FPR	1.7	2.1	1.7	1.7	1.7	1.7
OPR	25	25	25	25	25	25
TET R (K)	3060 (1700)	3240 (1800)	2880 (1600)	2880 (1600)	2970 (1650)	2970 (1650)
F lbf (N)	12,300 (55,000)	13,500 (60,000)	4000 (18,000)	4000 (18,000)	9000 (40,000)	7900 (35,000)
SFC lb/lfb h (mg/N s)	0.54 (15.0)	0.54 (15.0)	0.90 (29.2)	1.17 (33.2)	0.68 (19.5)	1.05 (30)
M_1	1.20 [1]	1.20 [1]	1.40 [2]	1.70 [2]	1.40 [2]	1.70 [2]
D_1 (m)	0.40 [1]	0.43 [1]	1.10 [2]	0.73 [2]	0.91 [2]	0.70 [2]
M_2	0.85 [1]	1.00 [1]				
D_2 (m)	0.70 [1]	0.67 [1]				

(1) perfect-expansion , (2) under-expansion

come larger than that of the coflow. This is possible if the jet nozzle lip extends downstream of the coflow nozzle lip as shown in Fig. 10(c). Compared to a more conventional adjustable-nozzle design, this configuration adds the complication and weight of the adjustable section upstream of the nozzle. In any case, this penalty appears to be much smaller than those introduced by other silencing systems (e.g. mixer-ejector). At cruise, two engines can produce a 8000 lbf thrust, sufficient for propelling a 65,000 lb aircraft with cruise $L/D \approx 10$. If the turbofan is converted to turbojet by diverting the fan stream to the core with a variable duct downstream of the fan, the resulting higher speed jet exhausts in a smaller adjustable nozzle. This solution can yield an overall weight saving advantage compared to the previous case. The cruise SFC of this configuration (1.17 lb/lbf h) is slightly better than that of the Concorde's engines (Olympus 593 with $SFC = 1.19$ lb/lbf h at same altitude and Mach 2.0 [14]) but worse than that of the mixed stream turbofan (0.9 lb/lbf h). Another drawback of this configuration is that the fan stages designed for fan flow rates at take-off are somewhat oversized for cruise conditions. These disadvantages can be mitigated using a cycle combining the characteristics of two cruise configurations above; i.e. a cruise cycle where part of the fan stream is diverted to the core and the remaining is mixed before expansion in the adjustable jet nozzle.

Transonic acceleration is another critical segment of the mission.

The extra thrust needed to overcome the high drag in this regime is usually obtained by reheating the exhaust stream. Because of its higher SFC, reheating should be kept at a minimum and possibly avoided. The last two columns of Table 4 indicate that both the mixed-stream turbofan and the turbojet discussed above are capable of doubling the cruise thrust during transonic regime without the need for reheating. This results in a $SFC = 0.68$ and 1.05 lb/lbf h, better than that of Concorde's engines (1.41 lb/lbf h) at the same conditions.

VII. Conclusions

The acoustics of supersonic jets surrounded by a coflow at conditions designed to prevent emission of Mach waves from the jet were investigated. Application of this method for designing quieter engines for a supersonic commercial aircraft was discussed. This is a summary of the main conclusions:

(a) Use of a coflow is a preferable means for suppressing the noise radiated from supersonic jets than reducing the jet speed by mixing the primary and secondary streams. It has been demonstrated that, at frequencies to which humans are more sensitive,

coflow at Mach Wave Elimination conditions can reduce the noise up to 16 dB in the direction of strongest emission and up to 8 dB in the lateral direction. Potential for further reductions exists by using asymmetric nozzle configurations which treat the noise directed towards the ground only.

(b) There is a flexibility in the choice of jet and coflow conditions capable of a good noise reduction.

(c) Jet and coflow combinations suitable for Mach Wave Elimination are compatible from an engine thermodynamic point of view and feasible using current technologies.

(d) An engine for propelling a supersonic business aircraft which applies the Mach Wave Elimination method, can be designed around the core of current military turbofan engines. It has been shown that the required modifications produce a moderate increase in the engine weight and complexity without penalizing performance.

References

[1] McLaughlin, D.K., Morrison, G.D., and Troutt, T.R., "Experiments on the Instability Waves in a Supersonic Jet and their Acoustic Radiation", *Journal of Fluid Mechanics*, Vol. 69, No. 11, 1975, pp.73-95.

[2] Troutt, T.R., and McLaughlin, D.K., "Experiments on the Flow and Acoustic Properties of a Moderate Reynolds Number Supersonic Jet", *Journal of Fluid Mechanics*, Vol. 116, March 1982, pp. 123-156.

[3] Tam, C.K.W. and Burton, D.E., "Sound Generated By Instability Waves of Supersonic Flows. Part 2. Axisymmetric Jets", *Journal of Fluid Mechanics*, Vol. 138, January 1984, pp.249-271.

[4] Tam, C.K.W., Chen , P., and Seiner, J.M., "Relationship Between Instability Waves and Noise of High-Speed Jets", *AIAA Journal*, Vol. 30, No.7, 1992, pp. 1747-1752.

[5] Seiner, J.M., Bhat, T.R.S, and Ponton, M.K., "Mach Wave Emission from a High-Temperature Supersonic Jet", *AIAA Journal*, Vol. 32, No. 12, 1994, pp. 2345-2350.

[6] Mitchell, B.E., Lele, S.K., and Moin, P., "Direct Computation of the Sound Generated by Subsonic and Supersonic Axisymmetric Jets", Report TF-66 of the Thermosciences Division, Department of Mechanical Engineering, Stanford University, Nov. 1995.

[7] Papamoschou. D., "Mach Wave Elimination from Supersonic Jets", *AIAA Journal*, Vol. 35, No. 10, 1997, pp. 1604-1611.

[8] Papamschou, D., "Method of Eliminating Mach Waves from Supersonic Jets," U.S. Patent No. 5590520, issued Jan. 7, 1997.

[9] Murakami, E., and Papamoschou, D., "PLIF Investigation of Coannular Supersonic Jets", AIAA paper No. 98-3015, June 1998.

[10] Papamoschou, D., Debiasi, M., "Noise Measurements in Supersonic Jets Treated with the Mach Wave Elimination Method", AIAA paper No. 98-0280, Jan. 1998.

[11] Debiasi, M., Papamoschou, D., "Acoustics of Under- and Over-Expanded Coaxial Jets", AIAA paper No. 99-0081, Jan. 1999.

[12] Papamoschou, D. and Bunyajitradulya, A. "Evolution of Large Eddies in Compressible Shear Layers", *Physics of Fluids*, Vol. 4, No. 3, 1997, pp. 756-765.

[13] Hill, P. and Peterson, C., "Mechanics and Thermodynamics of Propulsion", 2nd Ed., Addison Wesley, 1992, New York, pp. 146-189.

[14] Calder, P.H. and Gupta, P.C., "Future SST Engines with particular reference to Olympus 593 Evolution and Concorde Experience", SAE Paper 751056, 1975.
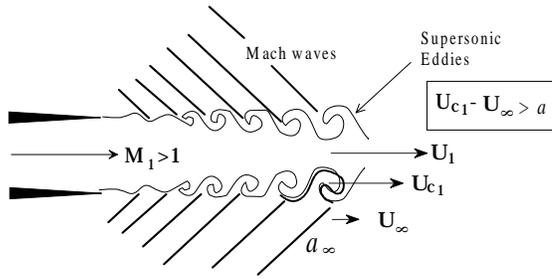
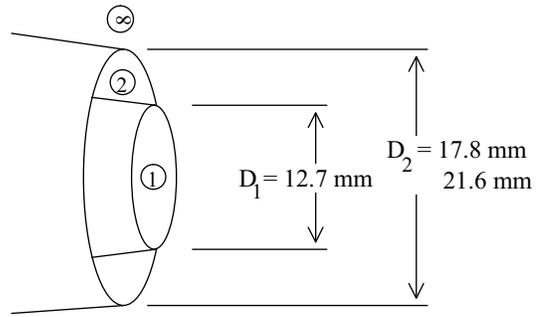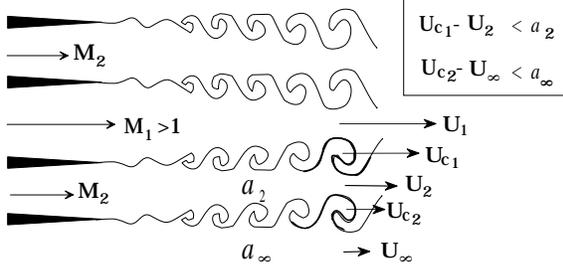Figure 1: Mach wave radiation in supersonic jets.

Figure 2: Principle of Mach Wave Elimination: creation of coflow adjacent to main jet so that all eddy motions become intrinsically subsonic.
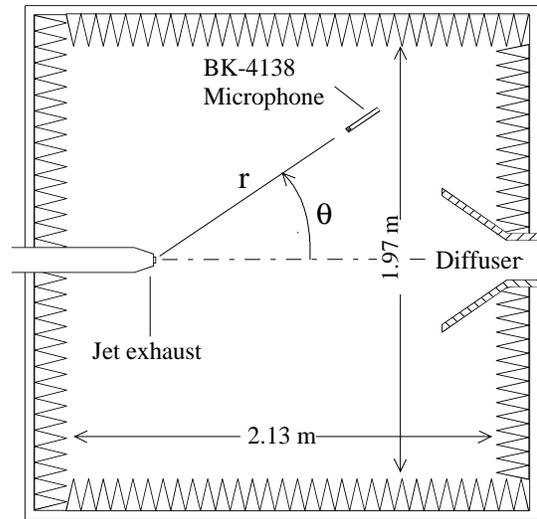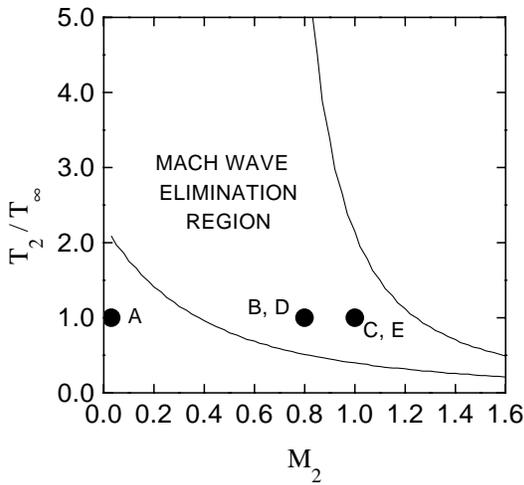

Figure 3: Mach Wave Elimination region for a jet with $M_1 = 1.2$ and $T_1/T_\infty = 2.5$; location of Cases A, B, C, D, and E is indicated.
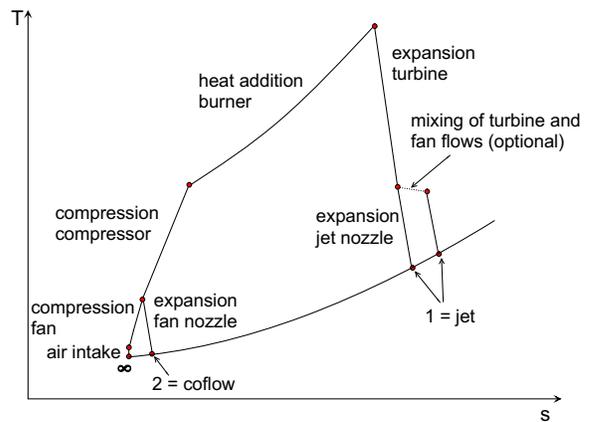

Figure 4: Coaxial supersonic jet facility.

Figure 5: Anechoic chamber and positioning of jet and microphone.

Figure 6: Brayton-Joule cycle for a turbofan/turbojet engine.

9
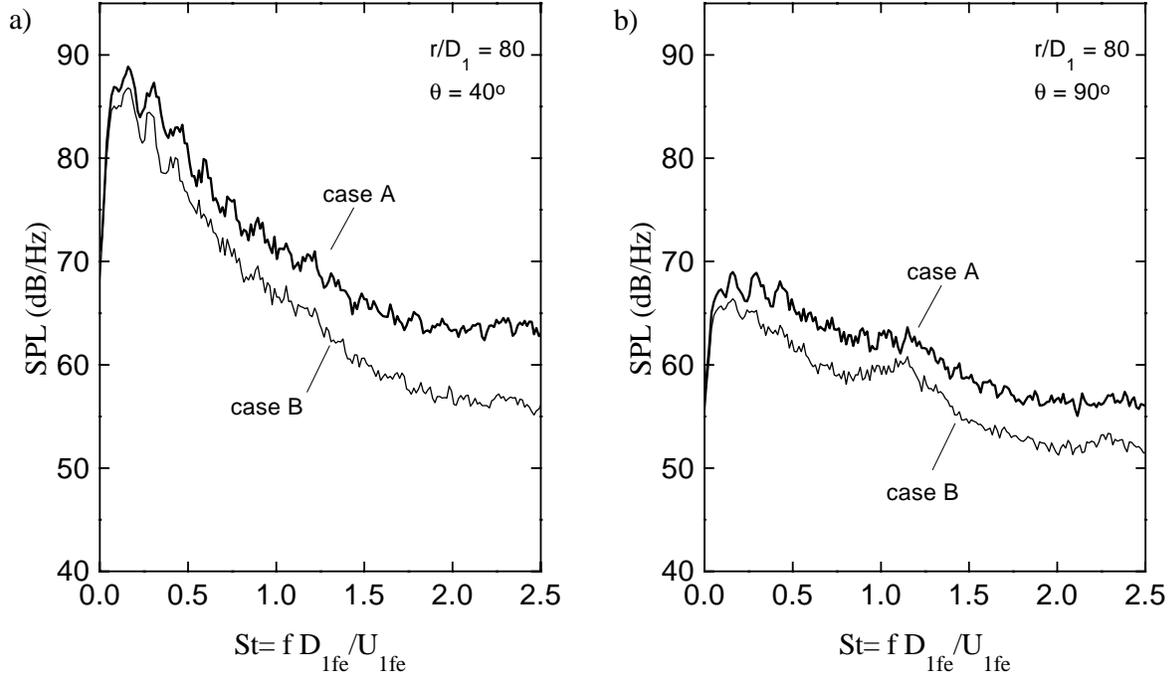
Figure 7: Far-field spectra of Case A (untreated jet with $M_1 = 1.2$, $U_1 = 700$ m/s) and Case B (same jet treated using a coflow with $M_2 = 0.8$, $U_2 = 300$ m/s, $D_2/D_1 = 1.4$ coflow): (a) peak OASPL direction; (b) lateral direction.
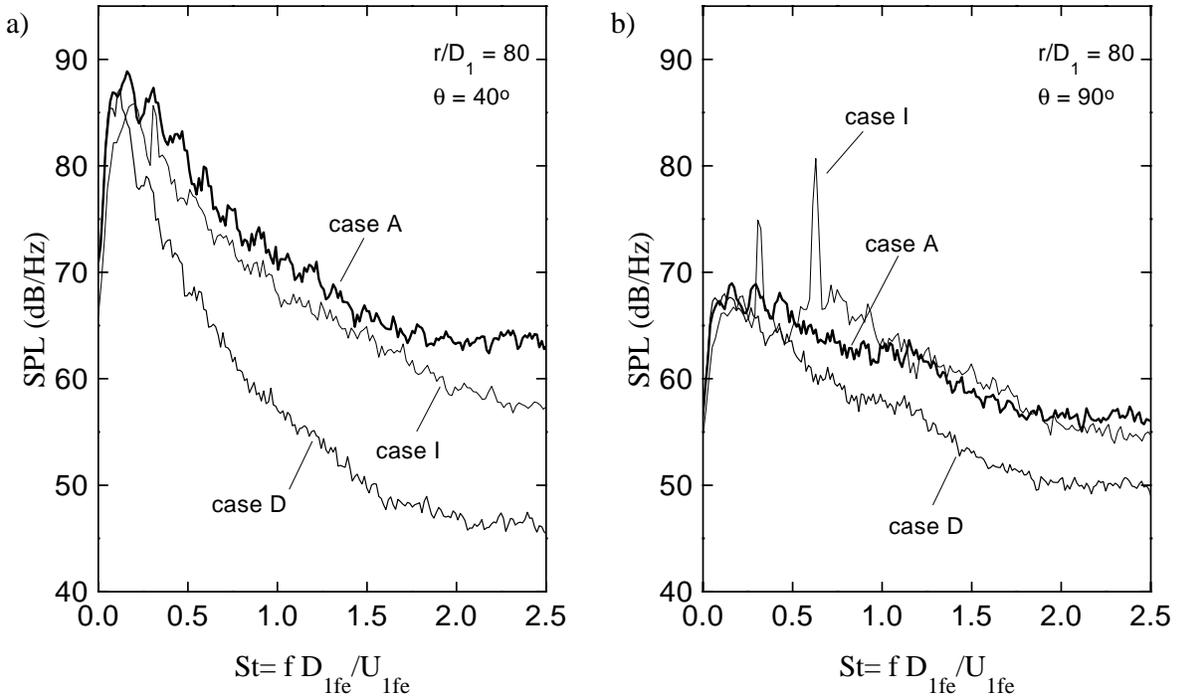

Figure 8: Far-field spectra of Case A (untreated jet with $M_1 = 1.2$, $U_1 = 700$ m/s), Case D (same jet treated using a coflow with $M_2 = 0.8$, $U_2 = 300$ m/s, $D_2/D_1 = 1.7$ coflow) and Case I (jet with $M_1 = 1.0$, $U_1 = 450$ m/s obtained mixing the jet and coflow of Case D before expansion in jet nozzle): (a) peak OASPL direction; (b) lateral direction.
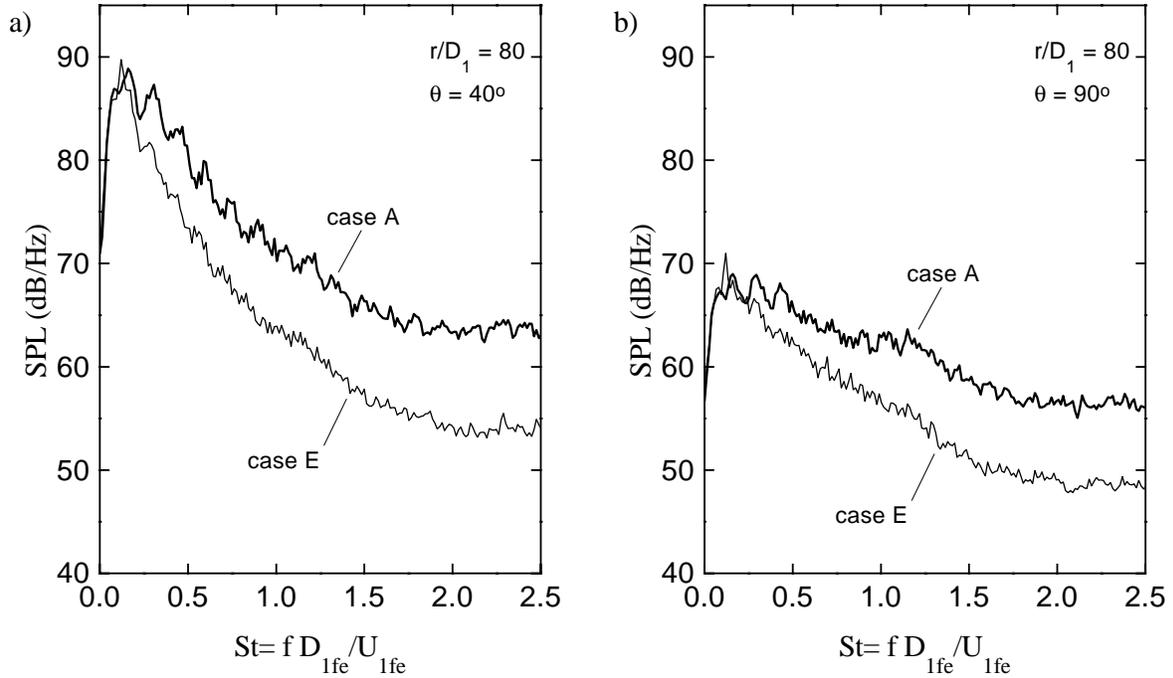
Figure 9: Far-field spectra of Case A (untreated jet with $M_1 = 1.2$, $U_1 = 700$ m/s) and Case E (same jet treated using a coflow with $M_2 = 1.0$, $U_2 = 350$ m/s, $D_2/D_1 = 1.7$ coflow): (a) peak OASPL direction; (b) lateral direction.
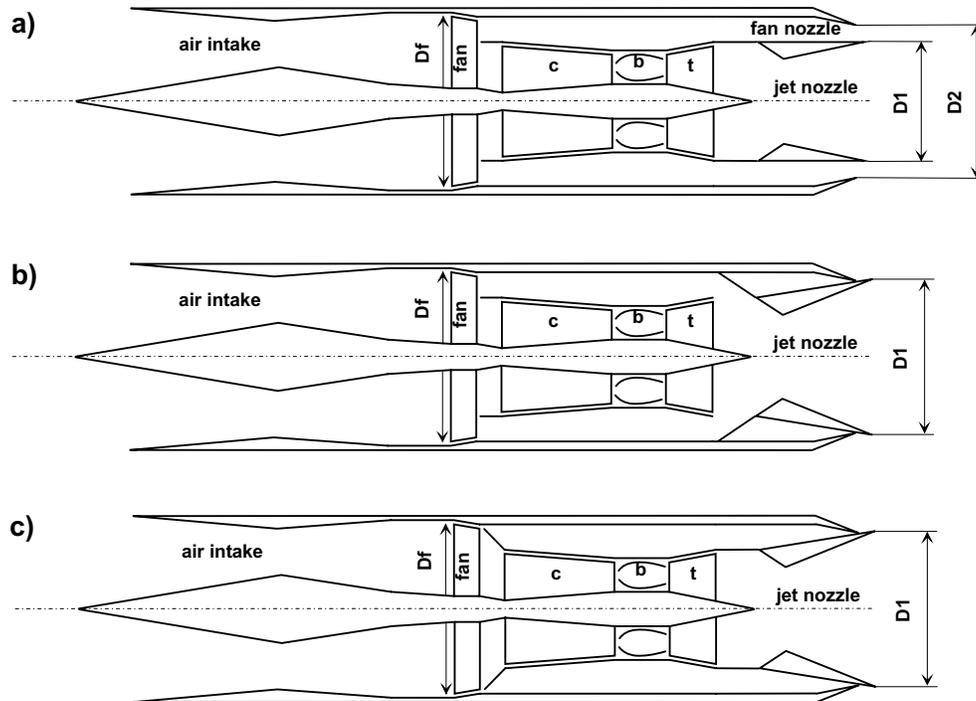

Figure 10: Mach Wave Elimination turbofan configurations: (a) at take-off; (b) with fan and core streams mixed at cruise; (c) converted to turbojet at cruise.